Analysis of the Young Open Cluster Trumpler 2 Using Gaia DR3 Data

S. Taşdemir[1]* , and T. Yontan[2]

[1]Istanbul University, Institute of Graduate Studies in Science, Programme of Astronomy and Space Sciences, 34116, Beyazit, Istanbul, Turkiye
[2]Istanbul University, Faculty of Science, Department of Astronomy and Space Sciences, 34119, Beyazit, Istanbul, Turkiye

ABSTRACT

We present an investigation of the open cluster Trumpler 2 using *Gaia* DR3 photometric, astrometric and spectroscopic data. 92 stars were identified as likely members of the cluster, with membership probabilities greater than 0.5. The mean proper-motion components of the cluster are derived as $(\mu_\alpha \cos \delta, \mu_\delta)$=(1.494 ± 0.004, −5.386 ± 0.005) mas yr^{-1}. By comparing the *Gaia* based colour-magnitude diagram with the PARSEC isochrones scaled to $z = 0.0088$, age, distance modulus and reddening are simultaneously estimated as $t = 110 \pm 10$ Myr, $\mu = 10.027 \pm 0.149$ mag and $E(G_{\rm BP} - G_{\rm RP}) = 0.452 \pm 0.019$ mag, respectively. The total mass of the cluster is estimated as 162 $M/M_\odot$ based on the stars with membership probabilities $P > 0$. The mass function slope is derived to be $\Gamma = 1.33 \pm 0.13$ for Trumpler 2. This value is in a good agreement with that of Salpeter. Galactic orbit analyses show that the Trumpler 2 orbits in a boxy pattern outside the solar circle and belongs to the young thin-disc component of the Galaxy.

Keywords: Galaxy: open clusters and associations; individual: Trumpler 2, Galaxy: Stellar kinematics, stars: Hertzsprung Russell (HR) diagram

1. INTRODUCTION

Open Clusters (OCs) are celestial objects consisting of stars bound to each under via mutual gravitational attraction. OCs are formed when a molecular cloud collapses. This means that the member stars of an OC formed under similar physical conditions and at a similar time. Hence, the stars that belong to the OCs have similar properties such as distance to Sun, metallicity and age. However stellar masses vary, leading to a range of stellar luminosities being observed in such clusters. These features make OCs valuable and interesting laboratories for understanding the formation and evolution of our Galaxy (Lada & Lada 2003).

The available information in the literature for the Trumpler 2 is as follows: Trumpler 2 ($\alpha = 02^{\rm h}36^{\rm m}55^{\rm s}.7, \delta = +55°54'18''$; $l = 137°.3863, b = −03°.9778$, J2000) is located at the Perseus Constellation. Since the cluster has low central concentration, it is classified in the Trumpler catalogue as II 2p (Trumpler 1930). Frolov et al. (2006) determined proper motion components of Trumpler 2 on 6 plates with a maximal epoch difference of 63 years by considering the positions of about 3,000 stars within the $B \sim< 16.25$ magnitude. By taking into account 148 stars assessed as the most probable cluster members, based on astrometric and photometric criteria, Frolov et al. (2006) obtained the colour-excess, distance modulus, distance and age

as 0.40 ± 0.06 mag, 10.50 ± 0.35 mag, 725 pc and 89 Myr, respectively. Zejda et al. (2012) determined the mean proper-motion components of 879 open clusters including Trumpler 2, based on 4 member stars in that cluster, as $(\mu_\alpha \cos \delta, \mu_\delta) = $ (1.0 ± 0.3, −4.6 ± 0.3) mas yr^{-1}. Dias et al. (2014) obtained the mean proper-motion components by using the U.S. Naval Observatory CCD Astrograph Catalogue (UCAC4; Zacharias et al. 2013) as $(\mu_\alpha \cos \delta, \mu_\delta) = $ (0.11 ± 1.48, −3.49 ± 2.23) mas yr^{-1}. They also identified 346 stars as members of Trumpler 2. Paunzen et al. (2014) studied chemically peculiar stars inside 10 open clusters including Trumpler 2. Moreover, it is confirmed that HD 16080 and BD+55 664 are members of Trumpler 2. As part of a survey of 1241 OCs, Joshi et al. (2016) derived the colour-excess, distance, age and total mass of Trumpler 2 as $E(B − V) = 0.321$ mag, $d = 670$ pc, $\log t = 7.925$ yr, and $M/M_\odot = 72.63 \pm 0.19$, respectively.

With the beginning of the *Gaia* era (Gaia Collaboration et al. 2016), the quality and accuracy of photometric, astrometric, and spectroscopic data have considerably taken a turn for the better. Cantat-Gaudin et al. (2018) investigated 1229 open clusters using the second data release of *Gaia* (*Gaia* DR2; Gaia Collaboration et al. 2018) and listed the mean astrometric parameters and membership probabilities of open clusters to characterize them. Cantat-Gaudin et al. (2018) identified 179 likely member stars ($P \geq 0.5$) in the direction of Trumpler 2, resulting

Table 1. Astrophysical parameters for Trumpler 2 compiled from the literature: Colour excesses ($E(B-V)$), distance moduli (μ_V), distances (d), iron abundances ([Fe/H]), age (t), proper-motion components ($\langle\mu_\alpha\cos\delta\rangle$, $\langle\mu_\delta\rangle$), radial velocities (V_γ) and references (Ref).

$E(B-V)$ (mag)	μ_V (mag)	d (pc)	[Fe/H] (dex)	t (Myr)	$\langle\mu_\alpha\cos\delta\rangle$ (mas yr^{-1})	$\langle\mu_\delta\rangle$ (mas yr^{-1})	V_γ (km s^{-1})	Ref
0.40±0.06	10.50±0.35	725	0.00	89	–	–	–	(01)
–	–	–	–	–	1.0±0.3	-4.6±0.3	–	(02)
–	–	–	–	–	0.11±1.48	-3.49±2.23	–	(03)
0.321	–	670	–	84	–	–	–	(04)
–	–	685^{+50}_{-44}	–	–	1.583±0.018	-5.352 ±0.015	–	(05)
–	–	685^{+50}_{-44}	–	–	1.583±0.018	-5.352 ±0.015	-4.12±0.09	(06)
$0.308^{+0.007}_{-0.006}$	10.289±0.021	736±7	0.00	91^{+14}_{-7}	–	–	–	(07)
–	–	694±23	–	81±5	1.574±0.273	-5.323±0.242	–	(08)
0.277	10.12	710	–	112	1.583±0.192	-5.352 ±0.167	–	(09)
0.307	–	685	-0.088±0.07	92	1.583±0.192	-5.352±0.167	-6.045±12.32	(10)
0.355±0.041	10.25±0.029	677±9	0.140±0.149	238±132	1.581±0.236	-5.343±0.193	-3.990±0.746	(11)
0.316	–	710	-0.262±0.106	110	1.58±0.19	-5.35±0.17	-4.16±0.02	(12)

(01) Frolov et al. (2006), (02) Zejda et al. (2012), (03) Dias et al. (2014), (04) Joshi et al. (2016), (05) Cantat-Gaudin et al. (2018), (06) Soubiran et al. (2018), (07) Bossini et al. (2019), (08) Liu & Pang (2019), (9) Cantat-Gaudin et al. (2020), (10) Zhong et al. (2020), (11) Dias et al. (2021), (12) Carrera et al. (2022)

is the proper-motion components being estimated as ($\mu_\alpha\cos\delta$, μ_δ) = (1.583 ± 0.018, -5.352 ± 0.015) mas yr^{-1} and distance d = 685^{+50}_{-14} pc. Soubiran et al. (2018) performed kinematic analyses for 861 open clusters using *Gaia* DR2 data, estimating the radial velocity V_γ = -4.12 ± 0.09 km s^{-1}, and space velocity components (U, V, W) = (-4.12 ± 0.08, -11.98 ± 0.08, -13.60 ± 0.06) km s^{-1} for Trumpler 2. Calculating the age, distance, distance modulus, and extinction values of 269 open clusters with the data obtained from the *Gaia* DR2 catalogue using the Bayesian statistical method, Bossini et al. (2019) determined the age of Trumpler 2 cluster as 91^{+14}_{-7} Myr. Liu & Pang (2019) used 86 member stars to calculate the mean proper-motion components, trigonometric parallaxes, and age. Accordingly, the values of the parameters as given as ($\langle\mu_\alpha\cos\delta, \mu_\delta\rangle$) = (1.574 ± 0.273, -5.323 ± 0.242) mas yr^{-1}, $\langle\varpi\rangle$ = 1.441±0.048 mas, and t = 81 ± 5 Myr. Cantat-Gaudin et al. (2020) obtained the astrometric and astrophysical parameters belonging to 2017 open clusters based on *Gaia* DR2 data. According to this study, the mean proper-motion components and parallaxes are calculated from 154 member stars as ($\langle\mu_\alpha\cos\delta, \mu_\delta\rangle$) = (1.583 ± 0.192, -5.352± 0.167) mas yr^{-1} and $\langle\varpi\rangle$ = 1.431 ± 0.058 mas, respectively. The recent study on the Trumpler 2 was carried out by Carrera et al. (2022). They performed high-resolution spectroscopic analyses and obtained metallicities for 41 stars with high membership probabilities in 20 open clusters including Trumpler 2. They determined metallicity value of Trumpler 2 as -0.262 ± 0.106 dex. Furthermore, analysing *Gaia* EDR3 astrometric data, Carrera et al. (2022) obtained the birth radius as 8.08 ± 0.05 kpc as well as the kinematic and dynamic orbital parameters of the cluster. The literature results are listed in Table 1 for ease of comparison.

2. DATA

2.1. Astrometric and Photometric Data

By using the high-quality data of the third data release of *Gaia* (*Gaia* DR3, Gaia Collaboration et al. 2022), we constructed the astrometric and photometric catalogue of the cluster. For this, we used the equatorial coordinates calculated by Cantat-Gaudin & Anders (2020) ($\langle\alpha,\delta\rangle$) = ($02^h36^m55^s.7, \delta$ = +55°54′18″) and take into account all stars located throughout the field of Trumpler 2 within the 50 arcmin region around the centre. Therefore it has been found that there are 121,569 stars with the stellar magnitudes between $7 < G \leq 23$ mag. The identification chart of stars ($50' \times 50'$) located in regions of Trumpler 2 is shown in Figure 1.

2.2. Photometric Completeness Limit and Photometric Errors

To calculate reliable structural and astrophysical parameters of open clusters, it is important to obtain the photometric completeness limit of the data. To determine the accurate parameter estimates for Trumpler 2, the photometric completeness limit of the stars is established by counting the stars corresponding to the G magnitudes. In Figure 2, the histogram shows the completeness limit as G = 20.50 mag which is indicative of an increase in the star count relative to the magnitude until this value and then decreases after it. In the following analyses, stars fainter than this value were excluded statistically and were not taken into account. The uncertainties in the *Gaia* DR3 data were accepted as interval errors and calculated mean G magnitudes with $G_{BP} - G_{RP}$ colour indices of stars in the cluster region as a function of G magnitude intervals. Considering G = 20.50
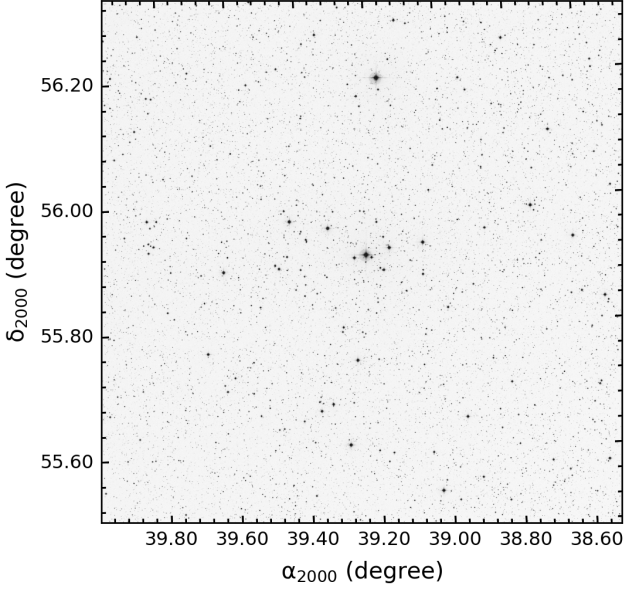
Figure 1. Identification chart of Trumpler 2. The field of view of the chart is $50' \times 50'$. North and East correspond with the up and left directions, respectively.
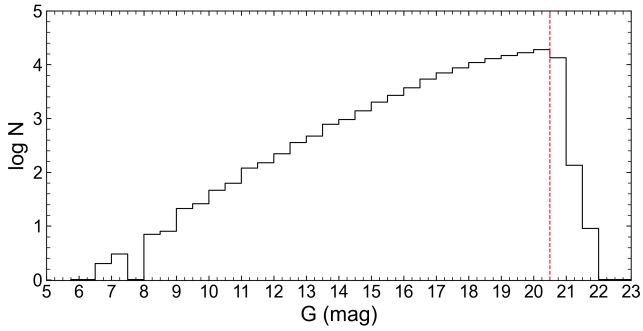

Figure 2. Histogram of number of stars with respect to G magnitude intervals for Trumpler 2. The red dashed-line indicates the faint limit magnitude of the cluster.

mag, the mean internal G magnitude and $G_{BP} - G_{RP}$ colour index were calculated as 0.007 and 0.142 mag at this limit, respectively. Mean errors of photometric data are listed in Table 2 as a function of G apparent magnitude. Also, Figure 3 presents the mean internal errors of G magnitudes and $G_{BP} - G_{RP}$ colour indices.

3. RESULTS

3.1. Structural Parameters of Trumpler 2

In order to investigate the extent of Trumpler 2 and determine its structural parameters, we performed Radial Density Profile (RDP) analysis. By using *Gaia* DR3 data within 50 arcmin, we divided the cluster area into many concentric rings from the central coordinates given by Cantat-Gaudin et al. (2020). For the calculation of the stellar density ($\rho(r)$), we used the stars within the $G \leq 20.5$ mag completeness limit and utilized the
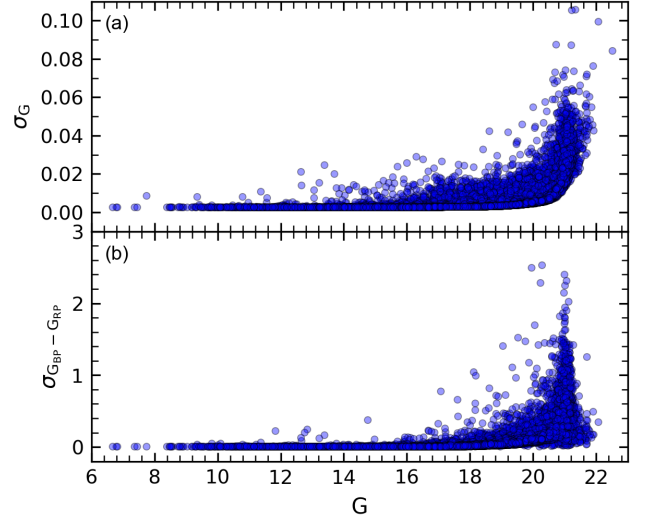

Figure 3. Mean photometric errors calculated for G apparent magnitude (a) and $G_{BP} - G_{RP}$ colour index for Trumpler 2.

Table 2. Mean internal photometric errors per magnitude bin in G apparent magnitude and $G_{BP} - G_{RP}$ colour index for Trumpler 2.

G (mag)	N	σ_G (mag)	$\sigma_{G_{BP}-G_{RP}}$ (mag)
(06, 14]	1839	0.003	0.006
(14, 15]	2056	0.003	0.006
(15, 16]	3930	0.003	0.006
(16, 17]	7566	0.003	0.009
(17, 18]	14083	0.003	0.017
(18, 19]	21699	0.003	0.038
(19, 20]	29495	0.005	0.081
(20, 21]	37454	0.010	0.208
(21, 23]	3447	0.027	0.430

equation of $R_i = N_i / A_i$ for each ith ring, where N_i and A_i are the number of stars falling into a given ring and the area of that ring, respectively. Uncertainties in the stellar density were calculated using the Poisson statistical measure $1/\sqrt{N}$, where N is the number of stars. Then, to plot the radial density profile we used the stellar density and fitted the RDP with the empirical King (1962) model defined by the following formula:

$$\rho(r) = f_{bg} + \frac{f_0}{1 + (r/r_c)^2} \tag{1}$$

In the equation, r denotes the radius of the cluster. The terms f_{bg}, f_0, r_c represent the background stellar density, the central stellar density and the core radius of Trumpler 2, respectively. Minimum χ^2 estimation was used in the RDP fitting process to estimate the f_{bg}, f_0 and r_c parameters which are listed in Table 3. The best-fit solution to the radial density profile is illustrated with a solid black line in Figure 4. The correlation coefficient of the King model (King 1962) with the best-fit model parameters to the data is $R^2 = 0.971$, which implies that the estimated structural parameters are well estimated.

Table 3. The structural parameters of the Trumpler 2 according to the King (1962) model analyses: (α, δ), f_0, f_{bg}, r_c, r_{lim}^{obs}, r_{lim}^{cal} and R^2 are equatorial coordinates, central stellar density, the background stellar density, the core radius, observational limiting radius, calculated limiting radius and correlation coefficient, respectively.

Cluster	α_{J2000} (hh:mm:ss.s)	δ_{J2000} (dd:mm:ss)	f_0 (stars arcmin^{-2})	f_{bg} (stars arcmin^{-2})	r_c (arcmin)	r_{lim}^{obs} (arcmin)	r_{lim}^{cal} (arcmin)	R^2
Trumpler 2	02:36:55.7	+55:54:18	1.55±0.33	12.59±0.02	2.48±1.09	12	11.7	0.971

Taking into account the visualisation of RDP, we determine the limiting radii (r_{lim}^{obs}) of cluster as 12. The structural parameters were derived as $f_{bg} = 12.59 \pm 0.02$, $f_0 = 1.55 \pm 0.33$ stars arcmin^{-2} and $r_c = 2.48 \pm 1.09$ arcmin (see also Table 3). To validate the precision of the observed limiting radii (r_{lim}^{obs}), equation given by Bukowiecki et al. (2011) is used as follow:

$$r_{lim} = r_c \sqrt{\frac{f_0}{3\sigma_{bg}} - 1}. \qquad (2)$$

From the equation, we calculated the theoretical limiting radius as 11.7 arcmin. It is obvious that theoretical and observed limiting radii values are in good agreement with each other.
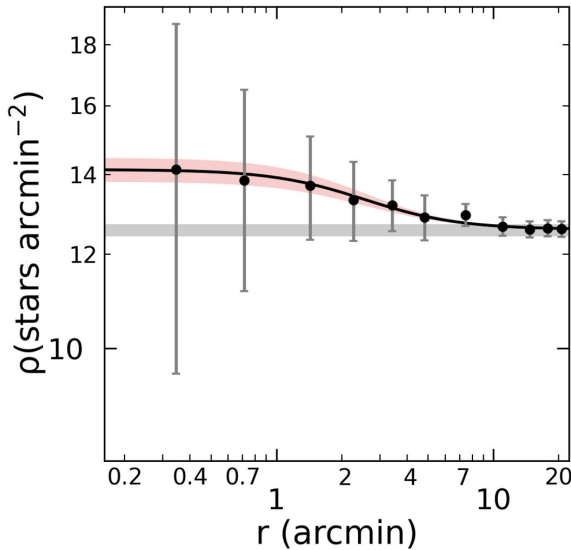

Figure 5. VPD of Trumpler 2 based on *Gaia* DR3 astrometry. The membership probabilities of the stars are identified with the colour scale shown on the right for the cluster. The zoomed-in panel inset represents the region of condensation for the cluster in the VPD. The mean proper-motion value of Trumpler 2 is shown by the intersection of the dashed blue lines.

Figure 4. The stellar density distribution of Trumpler 2. The fitted black curve shows the RDP profile of King (1962), whereas the horizontal grey band represents the background stellar density. The 1σ King fit uncertainty is pictured by the red-shaded area.

3.2. Membership Probabilities of Stars

As open clusters are located within the Galactic plane, they are highly contaminated by foreground and background stars. This situation makes it necessary to separate cluster members from field stars for determining reliable astrophysical parameters of the studied cluster. As the member stars of an OC form under similar physical conditions, they have similar vectorial movements in space. These properties make proper-motion components functional information to distinguish cluster members
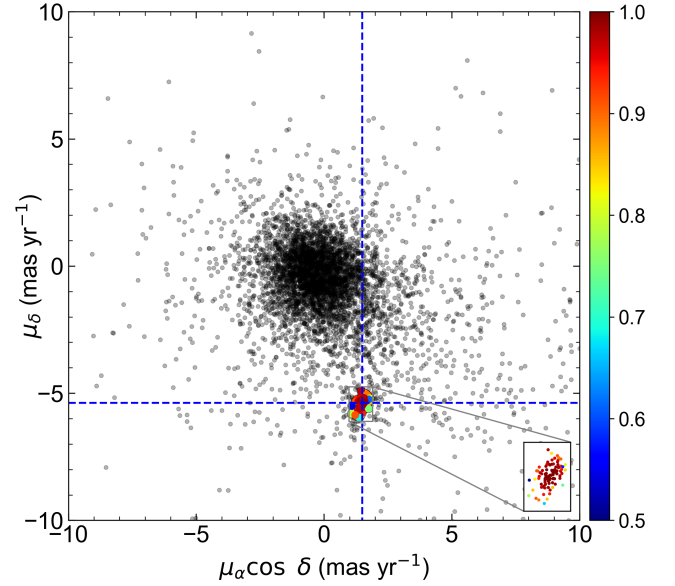
from the field stars (Bisht et al. 2020). The high accuracy of *Gaia* DR3 data (Gaia Collaboration et al. 2022) leads to reliable results for membership analyses. To determine the membership probabilities (P) of stars in the direction of Trumpler 2, we used the membership determination method known as Photometric Membership Assignment in Stellar Clusters (UPMASK, Krone-Martins & Moitinho 2014) on the *Gaia* DR3 astrometric data. Many researchers have previously utilized this method (Cantat-Gaudin et al. 2018, 2020; Castro-Ginard et al. 2018, 2019, 2020; Banks et al. 2020; Akbulut et al. 2021; Wang et al. 2022; Yontan 2023). UPMASK is a clustering method which is defined as k-means. The method allows the detection of similar groups of stars according to their proper-motion components and trigonometric parallax, providing statistical probability values for membership of these groups. We used each detected stars' astrometric measurements (α, δ, $\mu_\alpha \cos \delta$, μ_δ, ϖ) as well as their uncertainties by running 100 iterations of UPMASK to set their membership probability values. Hence, we identified 92 stars for Trumpler 2 as the most probable member stars with membership probabilities $P \geq 0.5$, brighter than the photometric completeness limits and located within the limited radius (r_{lim}^{obs}) described above.
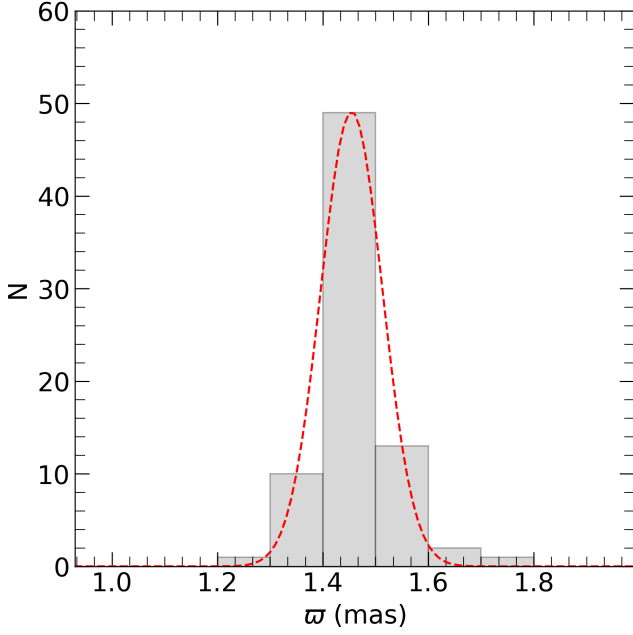
Figure 6. Histogram of mean trigonometric parallax estimation of Trumpler 2 from the most probable members ($P \geq 0.50$). Red dashed line shows the fitted Gaussian function.

We constructed the Vector-Point Diagram (VPD), which consists of proper-motion components of the stars, to investigate the most probable cluster member stars, as shown in Figure 5. It can be seen from the figure that Trumpler 2 is clearly distinguished from the foreground and background stars. In Figure 5, the intersection of the blue dashed lines represents the mean proper-motion values obtained from the most probable member stars ($P \geq 0.5$). The mean proper-motion components of Trumpler 2 are found as ($\mu_\alpha \cos\delta$, μ_δ)=(1.494 ± 0.004, −5.386 ± 0.005) mas yr^{-1}. Also, using these member stars we plotted the trigonometric parallax histogram and calculated the mean value by fitting the Gaussian functions to the distributions as shown in Figure 6. Thus, we estimated the mean trigonometric parallax value as ϖ=1.455±0.059 mas for the cluster. We transformed the mean trigonometric parallax to the trigonometric parallax distance (d_ϖ) by using the linear equation of $d(\mathrm{pc}) = 1000/\varpi$ (mas) and estimated the value as $d_\varpi = 687 \pm 27$ pc. This result is in a good agreement with the results determined in the *Gaia* era by different researchers (for a detailed comparison see Table 1).

3.3. Astrophysical Parameters of Trumpler 2

Colour-magnitude diagrams (CMDs) are essential tools to obtain basic astrophysical parameters such as age, distance modulus, reddening and metallicity of open clusters. These diagrams allow identification of a cluster's main sequence, turn-off point, and giant members as well as the determination of reliable cluster parameters. In the current study, considering the morphology of the most probable ($P \geq 0.5$) cluster members on the *Gaia* based CMD, we estimated age, distance moduli

and reddening simultaneously, whereas the metallicity [Fe/H] was adopted with the value of [Fe/H]=−0.262 ± 0.106 dex as given by Carrera et al. (2022). To derive the age, distance moduli and reddening of Trumpler 2, we applied PARSEC stellar isochrones (Bressan et al. 2012) to the observed CMD and obtained the best fit. We used the PARSEC[1] isochrones corresponding to *Gaia* Early Data Release 3 (EDR3) photometric passbands (Riello et al. 2021).

We transformed the adopted metallicity [Fe/H]=−0.262 ± 0.106 dex) to the mass fraction z for the selection of isochrones as well as for determination of astrophysical parameters. For the transformation, we applied the analytic expressions of Bovy[2] suitable for PARSEC isochrones (Bressan et al. 2012). The expressions are given as follow:

$$z_{\mathrm{x}} = 10^{[\mathrm{Fe/H}]+\log\left(\frac{z_\odot}{1-0.248-2.78 \times z_\odot}\right)}, \qquad (3)$$

and

$$z = \frac{(z_{\mathrm{x}} - 0.2485 \times z_{\mathrm{x}})}{(2.78 \times z_{\mathrm{x}} + 1)}. \qquad (4)$$

where z_{x} and $z_\odot$ indicate intermediate values where solar metallicity $z_\odot$ was accepted as 0.0152 (Bressan et al. 2012). We derived $z = 0.0088$ for Trumpler 2.

To determine the age, distance moduli and reddening of the cluster, we constructed a $G \times (G_{\mathrm{BP}} - G_{\mathrm{RP}})$ CMD and fitted selected isochrones by visual inspection, according to the most probable ($P \geq 0.5$) main sequence, turn-off, and giant member stars. Before the selection of isochrones, we scaled them to the mass fraction z, as determined above. This procedure indicated that the *Gaia*-based colour excess for Trumpler 2 is $E(G_{\mathrm{BP}} - G_{\mathrm{RP}})= 0.452 \pm 0.019$ mag. To compare with literature studies more accurately, we transformed this value to the *UBV*-based colour excess $E(B - V)$ by employing the equation $E(G_{\mathrm{BP}} - G_{\mathrm{RP}}) = 1.41 \times E(B - V)$ as given by Sun et al. (2021). Hence, we find the value as $E(B - V)$=0.320 ± 0.013 mag which is compatible with the results given by Joshi et al. (2016), Bossini et al. (2019), Zhong et al. (2020) and Carrera et al. (2022) within the errors (see Table 1).

The PARSEC isochrones with different ages of log(age) = 8.00, 8.04 and 8.08 with $z = 0.0088$ were superimposed to the observed $G \times (G_{\mathrm{BP}} - G_{\mathrm{RP}})$ CMD as shown in Figure 7. The overall fit is acceptable for log(age) = 8.04 to the most probable members ($P \geq 0.5$), corresponding to the age of Trumpler 2 being $t = 110 \pm 10$ Myr. The derived age value is compatible with the values given by Bossini et al. (2019), Zhong et al. (2020) and Cantat-Gaudin et al. (2020) within the formally stated errors (Table 1). The estimated distance modulus $\mu = 10.027 \pm 0.149$ mag corresponds to an isochrone distance

---

[1] http://stev.oapd.inaf.it/cgi-bin/cmd

[2] https://github.com/jobovy/isodist/blob/master/isodist/Isochrone.py
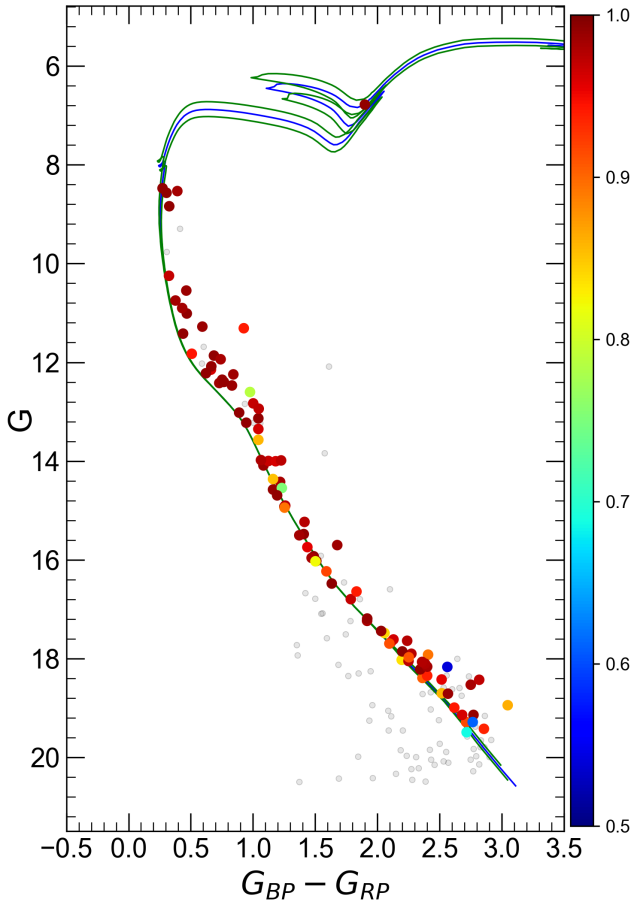
Figure 7. Colour-magnitude diagram for the studied cluster Trumpler 2. Different colour scales show the membership probabilities of the most probable cluster members. The scales of memberships are represented on colourbars to the right. Grey-coloured dots identify the stars with probabilities $P < 0.5$. The best fitting PARSEC isochrones and their errors are shown as the blue and green lines, respectively. Superimposed isochrone ages match to 110 Myr for Trumpler 2

from Sun as $d_{\rm iso} = 686 \pm 49$ pc. The errors in distance modulus and isochrone distance were calculated from the relations presented in Carraro et al. (2017). These relations take into account the photometric magnitude and colour excess with their uncertainties. The estimated isochrone distance is in a good agreement with the values given by different researchers (see Table 1) as well as with the value of trigonometric parallax distance $d_\varpi = 687 \pm 27$ pc calculated in this study.

Moreover, we derived Galactocentric coordinates $(X, Y, Z)_\odot$ of Trumpler 2, where X, Y, and Z are directions toward the Galactic centre in the Galactic disc, the Galactic rotation and the Galactic north pole, respectively. We used isochrone distance, Galactic longitude and latitude of the cluster and calculated these values as $(X, Y, Z)_\odot = (-504, 464, -48)$ pc. These findings are in fair agreement with the results of Cantat-Gaudin et al. (2020) (see also Table 4).

4. SPACE VELOCITIES AND GALACTIC ORBITAL PARAMETERS

Kinematic and dynamical orbit analyses of open clusters are important to understand the birth radii and Galactic populations of these objects (Yontan 2023). In this study we performed orbital integration analyses and obtained the Galactic orbital parameters for Trumpler 2. To do this, we used MWPOTENTIAL2014 in the Galactic dynamics library GALPY[3] package of Bovy (2015) which is written in Python. The MWPOTENTIAL2014 model represents the sum of three-component potentials: the spherical bulge as described in Bovy (2015), the Galactic disc as defined by Miyamoto & Nagai (1975) and the massive, spherical dark-matter halo as defined by Navarro et al. (1996). The Galactocentric distance and orbital velocity of Sun were taken as $R_{\rm gc} = 8$ kpc and $V_{\rm rot} = 220$ km s^{-1}, respectively (Bovy 2015; Bovy & Tremaine 2012). The distance from the Galactic plane of the Sun was accepted as 25 ± 5 pc (Jurić et al. 2008).

For the complete integration of the orbit, radial velocity information is one of the necessary parameters to be known. We used the available *Gaia* DR3 radial velocities of the stars to determine mean radial velocity and its uncertainty for Trumpler 2. To do this, we took into account the most probable member stars with membership probabilities $P \geq 0.9$, and the number of these stars are 33. The calculation was based on the weighted average of stars' radial velocities (for equations see Soubiran et al. 2018). Thus, the mean radial velocity was obtained as $V_\gamma = -4.48 \pm 1.11$ km s^{-1}. The literature mean radial velocity findings for Trumpler 2 (see also Table 1) are -4.12 ± 0.09 (Soubiran et al. 2018), -6.045 ± 12.32 (Zhong et al. 2020), -3.990 ± 0.746 km s^{-1} (Dias et al. 2021) and -4.16 ± 0.02 km s^{-1} (Carrera et al. 2022). The mean radial velocity obtained in this study for Trumpler 2 is within 1 km s^{-1} of the values are presented in these literature studies. To carry out the orbit integration, we provide the following parameters as input: the central equatorial coordinates ($\alpha = 02^{\rm h}36^{\rm m}55^{\rm s}.7$, $\delta = +55^{\rm o}54'18''$) taken from Cantat-Gaudin et al. (2020), the mean proper-motion components ($\mu_\alpha \cos \delta = 1.494 \pm 0.004$, $\mu_\delta = -5.386 \pm 0.005$ mas yr^{-1}) estimated in Section 3.2, the isochrone distance ($d_{\rm iso} = 686 \pm 49$ pc) from Section 3.3, and the radial velocity ($V_\gamma = -4.48 \pm 1.11$ km s^{-1}) calculated in the study (see also Table 4).

We integrated the cluster orbit forward with an integration step of 1 Myr up to 2.5 Gyr in order to derive the cluster's possible current location. Figure 8a shows the 'side view' of the cluster on $Z \times R_{\rm gc}$ plane, which indicates the distance from the Galactic plane and the Galactic centre. To estimate the possible birth radius of the Trumpler 2, we performed orbit analyses in the past epoch across a time period equal to its age (110 Myr). The integration procedure was limited to the cluster's age as the potential based uncertainties in time, as

---

[3] See also https://galpy.readthedocs.io/en/v1.5.0/

well as the additional errors in the distance, proper-motion components and radial velocity influence the reliability of the results (Gaia Collaboration et al. 2018; Sariya et al. 2021). Figure 8b indicates the distance of the cluster on the and $R_{gc} \times t$ plane with time. In the figure, the effect of uncertainties in the input parameters on the orbit of Trumpler 2 is represented. The results show that Trumpler 2 has an uncertainty of about 0.08 kpc for its possible birth-radius. These results also indicated that the cluster was formed outside the solar vicinity with a birth radius of 8.71 kpc.

Orbit integration resulted in the following derivation for Trumpler 2: apogalactic (R_a = 8752 ± 107 pc) and perigalactic (R_p = 8438 ± 10 pc) distances, eccentricity (e = 0.018 ± 0.007), the maximum vertical distance from Galactic plane (Z_{max} = 101 ± 17 pc), space velocity components ($U, V, W = -3.71 \pm 1.32, -12.08 \pm 0.10, -13.81 \pm 1.07$ km s^{-1}), and orbital period (P_{orb} = 242 ± 1 Myr). Taking into account the space velocity component values $(U, V, W)_\odot$ = (8.83 ± 0.24, 14.19 ± 0.34, 6.57 ± 0.21) km s^{-1} of Coşkunoğlu et al. (2011), we applied a Local Standard of Rest (LSR) correction to the (U, V, W) components of Trumpler 2. Hence, we derived the LSR corrected space velocity components as $(U, V, W)_{LSR}$ = (5.12 ± 1.34, 2.11 ± 0.35, −7.24 ± 1.09) km s^{-1}. Using these LSR results, we estimated the total space velocity as S_{LSR} = 9.12 ± 1.76 km s^{-1}, which is compatible with the velocity value given for young thin-disc stars (Leggett 1992). Perigalactic and apogalactic distances show that orbit of Trumpler 2 is completely outside the solar circle (Figure 8a). The cluster rises a maximum distance above the Galactic plane
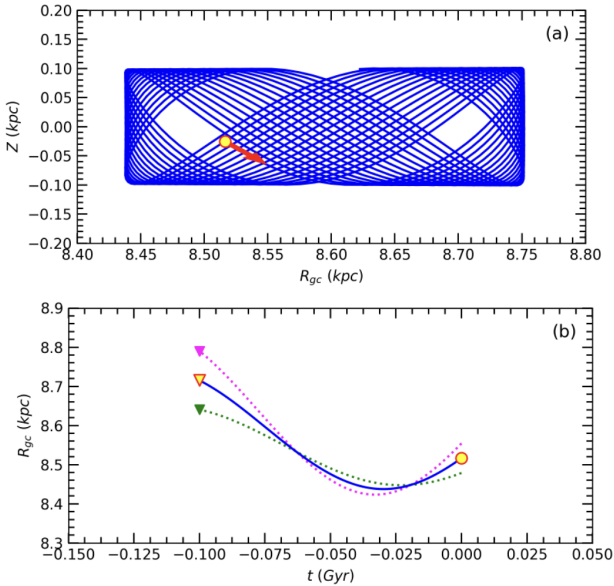
at Z_{max} = 101 ± 17 pc, indicating that Trumpler 2 belongs to the thin-disc component of the Milky Way (Bilir et al. 2006a,b, 2008).

5. LUMINOSITY AND MASS FUNCTIONS

The distribution of stellar brightness in an open cluster is known as its Luminosity Function (LF). The luminosity function and mass function (MF) are related by well-known mass-luminosity relationships. The correlation between the absolute magnitude and mass of the main-sequence stars can be estimated by a high-degree polynomial equation from the best-fitted age isochrone of the cluster. We used main-sequence stars with probabilities $P > 0$, located inside the limiting radius obtained in the study (r_{lim}^{obs} = 12 arcmin) and within the magnitude range $10 \leq G \leq 19.5$ magnitudes to investigate the LF of Trumpler 2. With these selection criteria, LF analyses were performed from 153 stars. We transformed apparent G magnitudes of the selected stars into the absolute M_G magnitudes using the distance modulus equation $M_G = G - 5 \times \log d + 1.8626 \times E(G_{BP} - G_{RP})$, where G, d and $E(G_{BP} - G_{RP})$ are apparent magnitude, isochrone distance, and colour excess that estimated for Trumpler 2 (see also Table 4). We plot as Figure 9 the LF histogram, with a bin width of 1 magnitude. It can be seen from the figure that the absolute magnitude ranges of the used stars lie within the $-2 < M_G < 11$ magnitude.

The MF was estimated from the LF through the mass-luminosity relation derived from the model isochrones (Bressan et al. 2012) based on the derived age and the previously adopted metallicity fraction (z) of the cluster. MF is described by the following expression:

$$\log(dN/dM) = -(1 + \Gamma) \times \log M + C. \quad (5)$$

where dN denotes the number of stars per unit mass dM, M states the central mass, C is the constant for the equation, and Γ is the slope of the MF.

We created a high-degree polynomial equation between the

Figure 8. The Galactic orbits and birth radii of Trumpler 2 in the $Z \times R_{gc}$ (a) and $R_{gc} \times t$ (b) planes. The filled yellow circle and triangles show the present-day and birth positions, respectively. Red arrow is the motion vector of Trumpler 2. The green and pink dotted lines show the orbit when errors in input parameters are considered, while the green and pink filled triangles represent the birth locations of the open cluster based on the lower and upper error estimates.
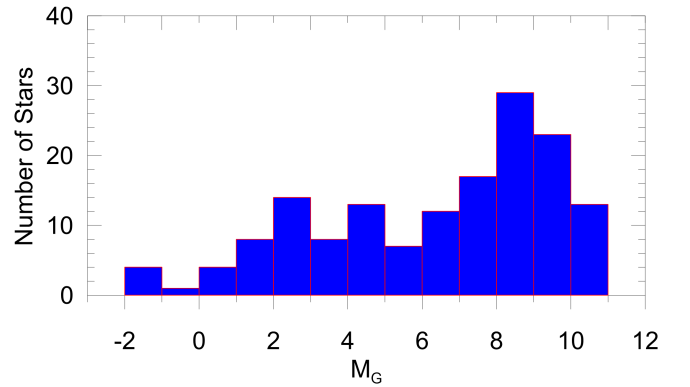

Figure 9. The luminosity function based on selected stars ($P > 0$) for Trumpler 2.

G-band absolute magnitudes and masses. Using this equation we transformed the observational absolute magnitudes M_G of the selected 153 stars ($P > 0$) into masses. With this process, we determined that the mass range of the 153 stars was inside $0.5 \leq M/M_\odot \leq 3.25$. Applying equation 5, we derived the MF slope value as $\Gamma = 1.33 \pm 0.13$ for the cluster, as shown in Figure 10.

In the study, the total mass of the cluster is also examined as a function of the membership probabilities of the stars, as shown in Figure 11. Figure 11a shows the total stellar mass with a bin width of 0.1 membership probabilities ($\Delta P = 0.1$), whereas Figure 11b represents the cumulative values of this distribution. Stars with probabilities $P > 0.9$ have a total mass of $106 M_\odot$, while stars with probabilities $P > 0$ have a total mass of $162 M_\odot$. Also, when considering the total mass of the stars with probabilities $P > 0.5$, the total mass of the cluster is
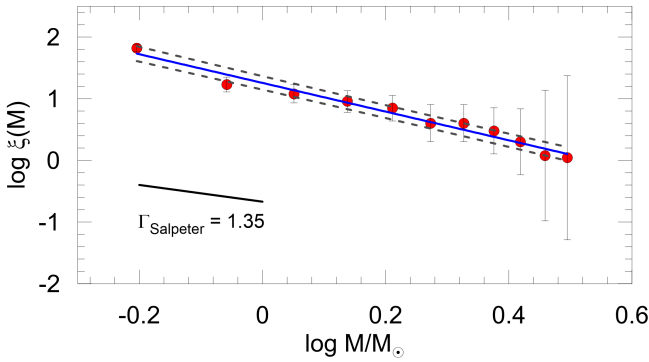

Figure 10. Mass function of Trumpler 2. Blue line indicates the calculated mass function of the cluster, whereas black dashed lines present the $\pm 1\sigma$ standard deviations. Black solid line shows the slope of Salpeter (1955).
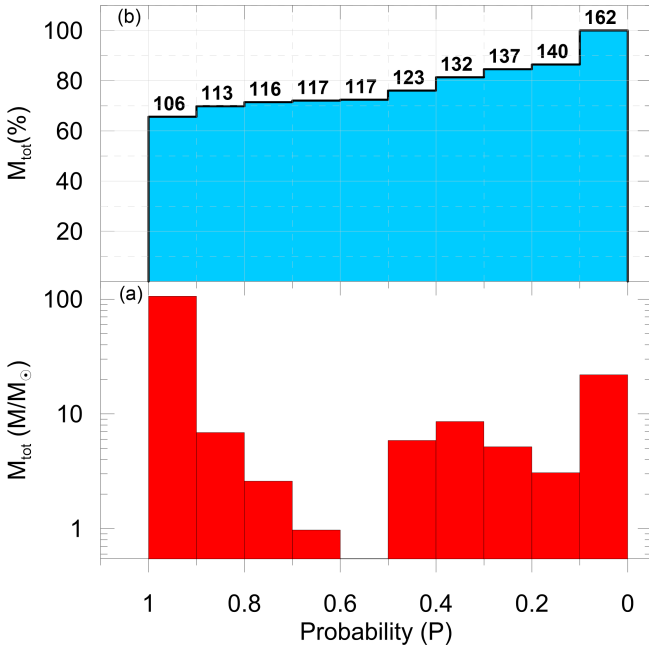

Figure 11. Total mass of Trumpler 2 based on membership probabilities (a) and their cumulative masses (b). The numbers above the bins represent the total mass of each bin in the histogram.

$117\ M/M_\odot$, corresponding to 72 per cent of the total mass of stars in all membership probabilities.

6. CONCLUSION

We presented photometric, astrometric, and kinematic analyses of open cluster Trumpler 2 using *Gaia* DR3 data. We identified 92 members as the most probable members with probabilities $P \geq 0.5$ in the direction of the cluster. These stars were used to estimate fundamental astrophysical and Galactic orbit parameters. We obtained age, distance modulus and reddening simultaneously from a *Gaia*-based CMD, whereas the metallicity is taken from the literature Carrera et al. (2022). The results are listed in Table 4. The main outcomes of current study are summarized as follows:

1. We derived structural parameters from the RDP analyses. Analyses concluded that the background stellar density, central stellar density and the core radius values of the cluster are $f_{bg} = 12.59 \pm 0.02$ stars arcmin^{-2}, $f_0 = 1.55 \pm 0.33$ stars arcmin^{-2} and $r_c = 2.48 \pm 1.09$ (arcmin), respectively. The limiting radius was determined by the visual eye from RDP fitting. It was adopted as the point where the RDP model matches with the background density level. Accordingly, the value of the limiting radius was concluded to be $r_{lim}^{obs} = 12$ arcmin.

2. On the basis of the VPD, we estimated mean proper-motion components as $(\mu_\alpha \cos\delta, \mu_\delta) = (1.494 \pm 0.004, -5.386 \pm 0.005)$ mas yr^{-1}.

3. The metallicity value ([Fe/H] = -0.262 ± 0.106 dex) of the cluster was taken from the study of Carrera et al. (2022) and transformed to the mass fraction $z = 0.0088$ to estimate age and distance modulus.

4. The *Gaia* based colour excess was estimated as $E(G_{BP} - G_{RP}) = 0.452 \pm 0.019$ mag by comparing the cluster CMD to the theoretical PARSEC isochrone (Bressan et al. 2012) with $z = 0.0088$. This value corresponds to a *UBV*-based colour excess to be $E(B - V) = 0.320 \pm 0.013$ mag via the use of expression $E(G_{BP} - G_{RP}) = 1.41 \times E(B - V)$ as given by Sun et al. (2021).

5. The isochrone fitting distance to the open cluster Trumpler 2 was derived as $d_{iso} = 686 \pm 49$ pc. This value is matched well by the distance obtained from the mean trigonometric parallax $d_\varpi = 687 \pm 27$ pc. The age was evaluated as $t = 110 \pm 10$ Myr by fitting the isochrone with $z = 0.0088$ scaled given by Bressan et al. (2012) to the observable CMD.

6. The mass function slope of Trumpler 2 was obtained as $\Gamma = 1.33 \pm 0.13$. This slope is in good agreement with the value of 1.35 given by Salpeter (1955). The total mass of Trumpler 2 is about $162\ M/M_\odot$.

7. Galactic orbit analyses showed that Trumpler 2 is orbiting in a boxy pattern outside the solar circle and belongs to the young thin-disc component of the Milky Way. Moreover, the birth-radius (8.71 ± 0.08 kpc) indicated that the cluster was formed outside the solar circle.

Table 4. Fundamental parameters of Trumpler 2.

Parameter	Value
$(\alpha, \delta)_{\mathrm{J2000}}$ (Sexagesimal)	02:36:55.7, +55:54:18
$(l, b)_{\mathrm{J2000}}$ (Decimal)	137.3863, -03.9778
f_0 (stars arcmin^{-2})	1.55±0.33
f_{bg} (stars arcmin^{-2})	12.59±0.02
r_{c} (arcmin)	2.48±1.09
r_{lim} (arcmin)	12
r (pc)	2.39
Cluster members ($P \geq 0.5$)	92
$\mu_\alpha \cos\delta$ (mas yr^{-1})	1.494 ± 0.004
μ_δ (mas yr^{-1})	-5.386 ± 0.005
ϖ (mas)	1.455 ± 0.059
d_ϖ (pc)	687 ± 27
$E(B-V)$ (mag)	0.320 ± 0.013
$E(G_{\mathrm{BP}} - G_{\mathrm{RP}})$ (mag)	0.452 ± 0.019
A_{G} (mag)	0.842 ± 0.035
[Fe/H] (dex)	$-0.262 \pm 0.106^*$
Age (Myr)	110 ± 10
Distance modulus (mag)	10.027 ± 0.149
Isochrone distance (pc)	686 ± 49
$(X, Y, Z)_\odot$ (pc)	$(-504, 464, -48)$
R_{gc} (kpc)	8.52
MF slope	1.33 ± 0.13
Total mass ($M/M_\odot$)	162
V_γ (km s^{-1})	-4.48 ± 1.11
U_{LSR} (km s^{-1})	5.12 ± 1.34
V_{LSR} (kms^{-1})	2.11 ± 0.35
W_{LSR} (kms^{-1})	-7.24 ± 1.09
S_{LSR} (kms^{-1})	9.12 ± 1.76
R_{a} (pc)	8752 ± 107
R_{p} (pc)	8438 ± 10
z_{max} (pc)	101 ± 17
e	0.018 ± 0.007
P_{orb} (Myr)	242 ± 1
Birthplace (kpc)	8.71 ± 0.08

*Carrera et al. (2022)

Peer Review: Externally peer-reviewed.

Author Contribution: Conception/Design of study - S.T., T.Y.; Conception/Design of study Data Analysis/Interpretation - S.T., T.Y.; Drafting Manuscript - S.T., T.Y.; Critical Revision of Manuscript - S.T., T.Y.; Final Approval and Accountability - S.T., T.Y.

Conflict of Interest: Authors declared no conflict of interest.

Financial Disclosure: Authors declared no financial support.

LIST OF AUTHOR ORCIDS

S. Taşdemir   https://orcid.org/0000-0003-1339-9148
T. Yontan   https://orcid.org/0000-0002-5657-6194

REFERENCES

Akbulut B., Ak S., Yontan T., Bilir S., Ak T., Banks T., Ulgen E. K., Paunzen E., 2021, Ap&SS, 366, 68

Banks T., Yontan T., Bilir S., Canbay R., 2020, Journal of Astrophysics and Astronomy, 41, 6

Bilir S., Karaali S., Ak S., Yaz E., Hamzaoğlu E., 2006a, New Astron., 12, 234

Bilir S., Karaali S., Gilmore G., 2006b, MNRAS, 366, 1295

Bilir S., Cabrera-Lavers A., Karaali S., Ak S., Yaz E., López-Corredoira M., 2008, Publ. Astron. Soc. Australia, 25, 69

Bisht D., Zhu Q., Yadav R. K. S., Durgapal A., Rangwal G., 2020, MNRAS, 494, 607

Bossini D., et al., 2019, A&A, 623, A108

Bovy J., 2015, ApJS, 216, 29

Bovy J., Tremaine S., 2012, ApJ, 756, 89

Bressan A., Marigo P., Girardi L., Salasnich B., Dal Cero C., Rubele S., Nanni A., 2012, MNRAS, 427, 127

Bukowiecki Ł., Maciejewski G., Konorski P., Strobel A., 2011, Acta Astron., 61, 231

Cantat-Gaudin T., Anders F., 2020, A&A, 633, A99

Cantat-Gaudin T., et al., 2018, A&A, 618, A93

Cantat-Gaudin T., et al., 2020, A&A, 640, A1

Carraro G., Sales Silva J. V., Moni Bidin C., Vazquez R. A., 2017, AJ, 153, 99

Carrera R., et al., 2022, A&A, 663, A148

Castro-Ginard A., Jordi C., Luri X., Julbe F., Morvan M., Balaguer-Núñez L., Cantat-Gaudin T., 2018, A&A, 618, A59

Castro-Ginard A., Jordi C., Luri X., Cantat-Gaudin T., Balaguer-Núñez L., 2019, A&A, 627, A35

Castro-Ginard A., et al., 2020, A&A, 635, A45

Coşkunoğlu B., et al., 2011, MNRAS, 412, 1237

Dias W. S., Monteiro H., Caetano T. C., Lépine J. R. D., Assafin M., Oliveira A. F., 2014, A&A, 564, A79

Dias W. S., Monteir H., Moitinho A., Lépine J. R. D., Carraro G., Paunzen E., Alessi B., Villela L., 2021, MNRAS, 504, 356

Frolov V. N., Ananjevskaja J. K., Jilinski E. G., Gorshanov D. L., Bronnikova N. M., 2006, A&A, 451, 901

Gaia Collaboration et al., 2016, A&A, 595, A1

Gaia Collaboration et al., 2018, A&A, 616, A1

Gaia Collaboration et al., 2022, arXiv e-prints, p. arXiv:2208.00211

Joshi Y. C., Dambis A. K., Pandey A. K., Joshi S., 2016, A&A, 593, A116

Jurić M., et al., 2008, ApJ, 673, 864

King I., 1962, AJ, 67, 471

Krone-Martins A., Moitinho A., 2014, A&A, 561, A57

Lada C. J., Lada E. A., 2003, ARA&A, 41, 57

Leggett S. K., 1992, ApJS, 82, 351

Liu L., Pang X., 2019, ApJS, 245, 32

Miyamoto M., Nagai R., 1975, PASJ, 27, 533

Navarro J. F., Frenk C. S., White S. D. M., 1996, ApJ, 462, 563

Paunzen E., Netopil M., Maitzen H. M., Pavlovski K., Schnell A., Zejda M., 2014, MNRAS, 564, A42

Riello M., et al., 2021, A&A, 649, A3

Salpeter E. E., 1955, ApJ, 121, 161

Sariya D. P., et al., 2021, AJ, 161, 101

Soubiran C., et al., 2018, A&A, 619, A155

Sun M., Jiang B., Yuan H., Li J., 2021, ApJS, 254, 38

Trumpler R. J., 1930, Lick Observatory Bulletin, 420, 154

Wang H., Zhang Y., Zeng X., Hu Q., Liu J., Qin M., Lü G., 2022, AJ, 164, 40

Yontan T., 2023, AJ, 165, 79

Zacharias N., Finch C. T., Girard T. M., Henden A., Bartlett J. L., Monet D. G., Zacharias M. I., 2013, AJ, 145, 44

Zejda M., Paunzen E., Baumann B., Mikulášek Z., Liška J., 2012, A&A, 548, A97

Zhong J., Chen L., Wu D., Li L., Bai L., Hou J., 2020, A&A, 640, A127